arXiv:1401.0819v2 [astro-ph.SR] 8 May 2014

General Relativistic Calculations for White Dwarf Stars

Arun Mathew and Malay K. Nandy

Department of Physics, Indian Institute of Technology Guwahati,

Guwahati 781 039, India.

Abstract

We restudy the properties of white dwarf stars composed of relativistic degenerate electron gas both in Newtonian and general relativity. Hence we investigate Mass-Radius relation for white dwarf stars by solving the Newtonian as well as Tolman-Oppenheimer-Volkoff equations for hydrostatic equilibrium considering the electron gas as non-interacting. We find that chandrasekhar's limiting mass of $1.452\,M_\odot$ for the Newtonian case is slightly modified to $1.397\,M_\odot$ in general gelativity for ${}^4_2$He (and ${}^{12}_6$C) white dwarf stars. The critical mass for ${}^{56}_{26}$Fe white dwarf stars is also calculated using general relativity, which is found to be $1.204\,M_\odot$. We also compare the critical densities for gravitational instability with the neutronization threshold. we find that ${}^4_2$He and ${}^{12}_6$C white dwarf stars are stable aganist neutronization with the critical value of $1.397\,M_\odot$ whereas the critical masses for stability are smaller due to neutronization for ${}^{16}_8$O, ${}^{20}_{10}$Ne, ${}^{24}_{12}$Mg, ${}^{28}_{14}$Si, ${}^{32}_{16}$S and ${}^{56}_{26}$Fe white dwarf stars. We obtain the maximum stable masses due to neutronization for these stars by solving the TOV equation corresponding to the central densities for neutronization thresholds.

PACS No.: 97.20.Rp.

1 Introduction

During the total solar eclipse of May 29, 1919, a group led by Eddington [1] confirmed the effect of general relativity in bending light rays around the sun. The experiment predicted the effect to be measurable for small stars of surface gravity 275 m/sec^2. Later in 1965, a second test for general relativity conducted by Pound and Rebka [2, 3] predicted that general relativistic effects (particularly, gravitational blue or red shift) are even recordable in the small gravitational field of the earth. These experiments clearly suggest that the effects of general relativity would be much more noticeable in the case of dense stars. It is therefore important to know what correction would follow due to Einstein's general theory of relativity if it were applied to dense stars like white dwarfs. As compared to Newtonian stars, the equation determining the hydrostatic equilibrium of a star changes drastically when the general theory of relativity is taken into account. In this paper we have studied how this change would modify the stellar structure of a few typical white dwarf stars. It appears that these effects may become important for large values of central density. However we find, in the case of a few white dwarfs, that the effect is small and it modifies the Chandrasekhar's limiting mass by a small amount.

White dwarfs are small faint stars having reached the end of their stellar evolution. The simplest

of them are composed mainly of helium at high temperature ($\sim 10^7$ K) and pressure. The thermal energy provided by the temperature is sufficiently large to ionize the helium atoms completely. The Fermi temperature ($\sim 10^{11}$ K) calculated from the electron density suggests that matter inside the star is highly degenerate [4]. The outward pressure created by the degenerate electron gas keeps the star from gravitational collapse.

After Dirac [5] formulated his Fermi-Dirac distribution in 1926, Fowler [6] treated the electron gas in Sirius-B as almost completely degenerate. He treated the electron gas as non-relativistic and found no limiting mass for the star. However, Anderson [7] and Stoner [8] considered the electron gas as relativistic and found the existence of a limiting density, although the treatments were heuristic. Chandrasekhar [9, 10, 11] obtained the limiting mass as $0.91\,M_\odot$ by treating the degenerate electron gas as relativistic. In 1934, Chandrasekhar [12] succeeded in formulating the theory of white dwarfs to full generality. He employed Newtonian gravity and an equation of state valid for the entire range of electron velocities, including relativistic velocities, of the degenerate Fermi gas to obtain the equation of hydrostatic equilibrium. He thus obtained the equations in the form of Lane-Emden equation with index 3 and solved the differential equations numerically to obtain the limiting mass of $1.44\,M_\odot$ (the Chandrasekar limit). In 1964, Chandrasekar [13] also consider the problem in the general relativistic framework and obtained the limiting mass as $1.4176\,M_\odot$. In 1965, Anand [14] studied the effect of rotation on a white dwarf star. He showed that the effect of rotation modifies the value of limiting mass to $1.704\,M_\odot$ implying an increase of 2.5% in Chandrasekhar's limiting mass. Qualitative arguments given by Landau and Lifshitz [15] suggests that the inter-particle Coulomb interaction is negligible in a white dwarf star. Later, using the method of Bohm and Pines [16], Singh showed that the correction to the electron density due to electron-electron interaction is small and can be treated as negligible [17].

In deriving the general relativistic equation of equilibrium for compact stars, Tolman [18] and Oppenheimer and Volkoff [19] showed how the Newtonian equation of hydrostatic equilibrium is modified into what is known as Tolman-Oppenheimer-Volkoff (TOV) equation. They considered the energy-momentum tensor for a perfect fluid in Einstein's field equation and solved for the metric for the interior of the star. It turned out to be a set of three differential equations in four unknown functions, which is incomplete unless provided with additional information, namely, the equation of state. While Tolman obtained the interior solution for a few different analytically tractable cases, Oppenheimer and Volkoff numerically solved those equations for massive neutron cores by taking the full equation of state treating it as a non-interacting Fermi gas.

In this paper we consider the hyrostatic equilibrium of white dwarf stars and obtain the mass-radius relationship by solving the Tolman-Oppenheimer-Volkoff equation. It is found, for large values of central density, that the Chandrasekhar's limit (in the Newtonian case) is slightly modified as a result of general relativity. Our calculation indicate that Chandrasekhar's limiting mass of $1.452\,M_\odot$ [20] is modified to $1.397\,M_\odot$ for ${}^4_2\mathrm{He}$ (and ${}^{12}_6\mathrm{C}$) white dwarf stars. The critical mass for ${}^{56}_{26}\mathrm{Fe}$ white dwarf stars is also calculated using general relativity, which is found to be $1.204\,M_\odot$.

We have also obtained the critical densities for gravitational instability directly from the solution of TOV equations without any approximation and comparethem with the neutronization thresholds. we find that ${}^4_2\mathrm{He}$ and ${}^{12}_6\mathrm{C}$ white dwarf stars are stable aganist neutronization with the critical value of $1.397\,M_\odot$ whereas the critical masses for stability are smaller due to neutronization for ${}^{16}_8\mathrm{O}$, ${}^{20}_{10}\mathrm{Ne}$,

$^{24}_{12}$Mg, $^{28}_{14}$Si, $^{32}_{16}$S and $^{56}_{26}$Fe white dwarf stars. We have also obtained the maximum stable masses due to neutronization for these stars by solving the TOV equation corresponding to the central densities for neutronization thresholds.

The paper is organized as follows. In Section 2, we outline the derivation of Tolman-Oppenheimer-Volkoff equation for a perfect fluid in equilibrium in general relativity. The problem of white dwarfs is taken up by considering the equation of state of cold degenerate electron gas in Tolman-Oppenheimer-Volkoff equation. The non-linear coupled differential equations so obtained are solved numerically in Section 3, where the equation following from Newtonian gravity are also solved for the sake of comparison. The mass-radius relationships obatined in the two cases are also compared. In Section 4, the instabilities due to gravitation and inverse beta decay are considered. The limiting masses at neutronization threshold are computed for a few relevant stars by solving the TOV equation. The numerical results are presented with a few relevant plots.

2 General Relativistic Treatment of White Dwarf Stars

The metric that describes the interior of a spherical symmetric star is given by [18, 19, 21, 22, 23, 24]

$$ds^2 = e^{\nu}dt^2 - e^{\lambda}dr^2 - r^2 d\theta^2 - r^2 \sin^2\theta \, d\phi^2 \tag{1}$$

where ν and λ are functions of r for the static case.

The matter inside the star is considered to be a perfect fluid with energy-momentum tensor

$$T_{\alpha\beta} = (\rho c^2 + p)u_\alpha u_\beta - p g_{\alpha\beta} \tag{2}$$

where ρ and p are the macroscopic mass-energy density and pressure respectively. For the line element given by Eq. (1), the non-zero components of the energy-momentum tensor are given by

$$T_{00} = \rho c^2 e^{\nu}, \quad T_{11} = p e^{\lambda}, \quad T_{22} = p r^2, \quad T_{33} = p r^2 \sin^2\theta \tag{3}$$

Einstein's field equations corresponding to the above line element and the energy-momentum tensor are given by

$$\begin{aligned} e^{-\lambda}\left(\frac{\lambda'}{r} - \frac{1}{r^2}\right) + \frac{1}{r^2} &= \frac{8\pi k}{c^2}\rho \\ e^{-\lambda}\left(\frac{\lambda'}{r} + \frac{1}{r^2}\right) - \frac{1}{r^2} &= \frac{8\pi k}{c^4}p \\ \frac{dp}{dr} &= -\frac{\nu'}{2}(\epsilon + p) \end{aligned} \tag{4}$$

where primes denote differentiation with respect to r. These three equations together with the equation of state of matter $\rho = \rho(p)$ determine the hydrostatic equilibrium for an isotropic general relativistic static fluid sphere.

From the above one can obtain the Tolman-Oppenheimer-Volkoff equation, namely

$$\frac{dp(r)}{dr} = -\frac{G\rho(r)m(r)}{r^2}\left[1 + \frac{p(r)}{\rho c^2}\right]\left[1 + \frac{4\pi p(r) r^3}{m(r)c^2}\right]\left[1 - \frac{2Gm(r)}{c^2 r}\right]^{-1} \tag{5}$$

where

$$m(r) = \int_0^r 4\pi\rho(r')r'^2 dr' \tag{6}$$

and the mass-energy density ρ has the form

$$\rho(r) = \rho_0(r)\left(1 + \frac{\epsilon(r)}{\rho_0(r)c^2}\right) \tag{7}$$

where ρ_0 and ϵ are the mass density and internal energy density respectively. Eqs. (5) and (6) together with the equation of state $\rho = \rho(p)$ determine the equilibrium configuration.

In a white dwarf star, the matter consists of electrons of rest mass m_e as a degenerate Fermi gas. The equation of state is given by the parametric forms

$$\rho = K_1 \sinh^3\frac{\xi}{4} f(\xi) \tag{8}$$

$$p = K_2(\sinh\xi - 8\sinh\frac{\xi}{2} + 3\xi) \tag{9}$$

where

$$f(\xi) = \left(1 + \frac{3m_e(\sinh\xi - \xi)}{32\mu_e H \sinh^3\frac{\xi}{4}} - \frac{m_e}{\mu_e H}\right)$$

$$\xi = 4\sinh^{-1}\frac{p_F}{m_e c}$$

$$K_1 = \frac{8\pi m_e^3 c^3 \mu_e H}{3h^3} \quad \text{and} \quad K_2 = \frac{\pi m_e^4 c^5}{12h^3}$$

where μ_e is the number of electrons per nucleon, H is proton mass, h the Planck's constant, p_F the Fermi momentum and c the speed of light. The above equations are valid for all values of electron velocities, including the extreme relativistic region.

Substituting Eqs. (8) and (9) in Eqs. (5) and (6), the following differential equations are obtained.

$$\frac{dm}{dr} = 4\pi r^2 K_1 \sinh^3\frac{\xi}{4} f(\xi) \tag{10}$$

$$\frac{d\xi}{dr} = -\frac{GK_1 \sinh^3\frac{\xi}{4} f(\xi) m(r)}{K_2(\cosh\xi - 4\cosh\frac{\xi}{2} + 3)r^2}\left[1 + \frac{K_2(\sinh\xi - 8\sinh\frac{\xi}{2} + 3\xi)}{K_1 c^2 \sinh^3\frac{\xi}{4} f(\xi)}\right]$$

$$\times\left[1 + \frac{4\pi K_2(\sinh\xi - 8\sinh\frac{\xi}{2} + 3\xi)r^3}{m(r)c^2}\right]\left[1 - \frac{2Gm(r)}{c^2 r}\right]^{-1} \tag{11}$$

We shall solve these equations numerically for white dwarf stars in the next section.

3 Numerical Integration

Eqs. (10) and (11) can be made dimensionless by introducing dimensionless variables $x = r/a$ and $u = m/b$ (which are referred to as dimensionless radius and mass, respectively). They reduce to the forms

$$\frac{du}{dx} = x^2 \sinh^3\left(\frac{\xi}{4}\right) f(\xi) \tag{12}$$

$$\frac{d\xi}{dx} = -\frac{\sinh^3\frac{\xi}{4} f(\xi) u(x)}{(\cosh\xi - 4\cosh\frac{\xi}{2} + 3)x^2}\left[1 + \frac{K_2(\sinh\xi - 8\sinh\frac{\xi}{2} + 3\xi)}{K_1 c^2 \sinh^3\frac{\xi}{4} f(\xi)}\right]$$
$$\times \left[1 + \frac{K_2(\sinh\xi - 8\sinh\frac{\xi}{2} + 3\xi)x^3}{K_1 u(x) c^2}\right]\left[1 - \frac{2Gb}{c^2 a}\frac{u(x)}{x}\right]^{-1} \tag{13}$$

We have chosen the values $a = 6.819 \times 10^7$ cm and $b = 7.8143 \times 10^{30}$ g so that the prefactors in equations (12) and (13) are normalized to unity. As analytical solution is not possible, we use numerical computation methods to integrate them simultaneously. Here we have employed fourth order Runge-Kutta method to integrate them. The solutions of these equations are computed for several initial values of ξ_0 at the centre of the star. Integration is carried out from the value $u = 0$, $\xi = \xi_0$ at $x = 0$ (centre) to $x = x_b$ (surface) where $\xi_b = 0$ (which makes $p = 0$), and $u = u_b$. Some of the results of the numerical intergration are given in Table 1 for $1.0 \leq \xi_0 \leq 20.0$.

In the limit $\xi \to \infty$, Eqs. (12) and (13) reduce to the simple forms

$$\frac{du}{dx} = \frac{3m_e}{64\mu_e H} x^2 e^{\xi} \tag{14}$$

Table 1: Mass, radius and central density for various ξ_0 for Helium white dwarf stars.

ξ_0	Mass M in $M_\odot$	Radius R in kilometers	$\log\rho_c$ (ρ_c in g/cm^3)	$\left(\frac{p_F}{m_e c}\right)$
1.0	0.084521	19746.389383	10.362801	0.252612
3.0	0.407264	10709.842055	13.903655	0.822317
5.0	0.761765	7341.770205	15.904258	1.175201
7.0	1.047059	5195.096775	17.569428	2.790414
9.0	1.233759	3643.887418	19.128266	4.691168
11.0	1.336404	2499.345585	20.650110	7.789352
13.0	1.383049	1669.260395	22.158909	12.875783
14.0	1.393032	1350.786443	22.911429	16.542627
15.0	1.396940	1086.495108	23.663461	21.248782
15.2	1.397133	1028.039843	23.851435	22.339407
16.0	1.396077	869.151828	24.415340	27.289917
17.0	1.391197	691.930580	25.167309	35.045574
18.0	1.382602	548.567085	25.919566	45.003011
19.0	1.370227	433.375828	26.672295	57.787816
20.0	1.353708	341.369215	27.425692	74.203211
∞	0.451680	51.33587	∞	∞

$$\frac{d\xi}{dx} = -\frac{m_e}{8\mu_e H}\frac{1}{x(x - 2C_1 u)}\left(u + \frac{m_e}{64\mu_e H} x^3 e^{\xi}\right) \tag{15}$$

where $C_1 = Gb/c^2 a$.

From Eqs. (8) and (9), the ratio of central pressure to the central mass-energy density for the limiting case $\xi_0 \to \infty$ turns out to be

$$\frac{p}{\rho c^2} = \frac{1}{3}$$

which represents a sphere of fluid with infinite density and pressure at the center. Eqs. (14) and (15) can be solved exactly and the solution is given by

$$u = \left(\frac{12\mu_e H}{m_e + 24C_1\mu_e H}\right) x \tag{16}$$

$$e^{\xi} = \frac{16\mu_e H}{m_e^2 + 24C_1\mu_e H}\left(\frac{1}{x^2}\right) \tag{17}$$

From the above solution we get the initial condition for the ξ_0 value. We use this initial value to integrate Eqs. (12) and (13) from $\xi = \xi_0$ (centre) to $\xi = 0$ (surface). This gives the last entry in Table 1.

As we wish to compare these results of numerical integration with the results following from Newtonian gravity, we also numerically integrate the following (Newtonian) equations.

$$\frac{du}{dx} = x^2 \sinh^3\frac{\xi}{4} \tag{18}$$

$$\frac{d\xi}{dx} = -\frac{u(x)\sinh^3\frac{\xi}{4}}{(\cosh\xi - 4\cosh\frac{\xi}{2} + 3)x^2} \tag{19}$$

The mass-radius relationship following from the numerical integrations of the TOV equations [Eqs. (12) and (13)] and the Newtonian equations [Eqs. (18) and (19)] are compared in Fig. 1. It is seen that the two mass-radius curves coincide for small values of ξ_0. This is due to the fact that the TOV equation reduces to the Newtonian equation for small values of central density as a result of negligible contribution of the internal energy and the smallness of the metric correction ($2GM/c^2R$). For small values of ξ_0, the equation of state reduces to the form $p = K\rho_0^{5/3}$ and the mass-radius relation goes like $M \sim R^{-3}$. We find that the linear part of the curve (the right part of the plot) has a slope approximately equal to -3.

For higher values of central density, the TOV curve starts to deviate from the Newtonian curve, as seen towards the left part of the plot. Thus, for large ξ_0, there is a departure from the non-relativistic $M \sim R^{-3}$ behavior for both Newtonian and TOV cases. We also find that the critical limiting mass is lower for the TOV case than the Newtonian case, the values being $1.397\,M_\odot$ and $1.452\,M_\odot$ respectively. The Newtonian value ($1.452\,M_\odot$) is the Chadrasekhar's limit (the well known value is $1.44\,M_\odot$) [20].

4 Stability of White Dwarf Stars

In this section we shall analyze the gravitational stability following directly from the solutions of Eqs. (12) and (13) using the conditions previously obtained in Ref. [26].

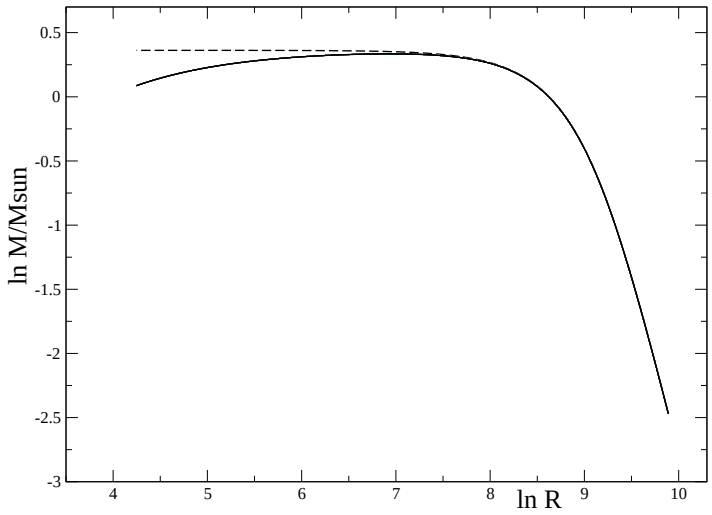

Figure 1: Mass-Radius relationships given by the TOV (full line) and the Newtonian (dashed line) equations for Helium white dwarf stars.

4.1 Gravitational Instability

The equilibrium configuration of the star is identified by the extremum in the energy-matter distribution curve. The total energy of the star was previously derived by adding corrections due to general relativity, which is given by [26]

$$E_T = E_{\rm int} + \Delta E_{\rm int} + E_{\rm Newt} + \Delta E_{\rm GTR} \tag{20}$$

where the first two terms correspond to the internal energy and the corresponding relativistic correction, the third term is the gravitational energy in Newtonian limit, and the fourth term is the correction due to general relativity. The hydrostatic Eqs. (18) and (19), based on Newtonian gravity, ignore the internal kinetic energy contribution and metic correction. Consequently the general relativistic effects are taken into account by adding first order corrections in the above eqaution as shown. Thus the above equation is an approximate expression for energy due to the general relativistic correction. This approximation is expected to be good when the mass-radius ratio in mertic correction is small.

Minimizing this energy gives the equilibrium condition $\frac{dE_T}{d\rho_c}\Big|_M = 0$. Minima and maxima correspond to stable and unstable equilibruim given by $\frac{\partial M}{\partial \rho_c} > 0$ and $\frac{\partial M}{\partial \rho_c} < 0$ respectivily. For $\frac{\partial M}{\partial \rho_c} < 0$, the electron degenerate pressure is smaller than the inward gravitational pull causing the star to collapse continuously. The onset of this collapse was obtained previously [26] by setting $\frac{\partial^2 E_T}{\partial \rho_c^2} = 0$. Thus the expression for density for onset of gravitational instability was calculated as

$$\rho_c^{\rm pre} = 2.646 \times 10^{10} \left(\frac{\mu_e}{2}\right)^2 {\rm g/cm}^3 \tag{21}$$

This is the central density at which the star becomes unstable aganist the gravitational pull. As noted above, this expression for the onset density of gravitaional instabilty is an approximation, as it

is based on Eq. (20). The critical values for the central density for a few white dwarf stars following from Eq. (21) are shown in Column 3 of Table 2.

In our present calculations, we take an alternative route to obtain the critical values for the central density. Thus we obtain the critical central density ρ_c from the solution of the full TOV equations [namely, Eqs. (12) and (13)] without making any approximations. Thus, our results are expected to be close to exact.

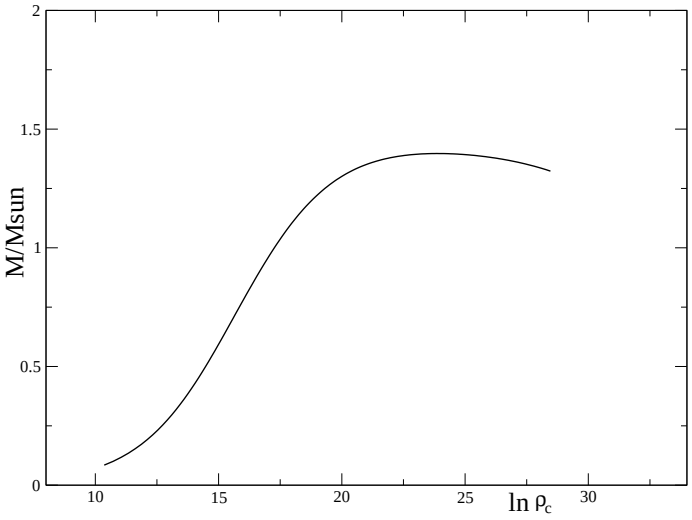

Figure 2: Dependence of mass M on central density ρ_c for Helium white dwarf stars.

The plot in Fig. 2 shows the dependence of mass on central density as a result of computation based on the TOV equation [(12) and (13)]. The mass of the star increases with increase in the central density until a maximum is reached beyond which it falls down. The positive slope ($\frac{\partial M}{\partial \rho_c} > 0$) corresponds to the stable portion whereas the negative slope ($\frac{\partial M}{\partial \rho_c} < 0$) to the unstable portion. The plot also predicts a maximum stable mass a white dwarf can achieve, which is very nearly $1.397\, M_\odot$. This corresponds to a central density of 2.359×10^{10} g/cm^3. For higher values of density, the star becomes unstable and collapses under its own gravitational pull.

Fig. 3 gives a plot of dependence of mass on ξ_0, where the mass on ordinate is in the units of $M_\odot$ ($= 1.98892 \times 10^{33}$ g). The plot shows increase in mass with increase in ξ_0 until a maximum mass is reached at $\xi_0 = 15.2$. After this value the curve steeps down to a value of $0.423\, M_\odot$ for $\xi_0 = 35.059$. The steep part of the curve shows the gravitational collapse of the white dwarf star against the degenerate pressure of the electron gas. Beyond the maxima the degenerate pressure is not sufficient to withstand the gravitational pull resulting in a collapse.

The occurence of a critical limiting mass can be clearly seen when we plot the mass M versus the radius R of the star on linear scales. This is shown in Fig. 4 for helium white dwarf stars, where the maxima is identified as the critical point (at a mass of about $1.397\, M_\odot$). The portion towards the right of the maxima corresponds to stable equilibrium, whereas that towards the left corresponds to instability. Thus the TOV equation gives a critical mass of $1.397\, M_\odot$ solar masses which is slightly smaller than that obtained by Chandrasekhar.

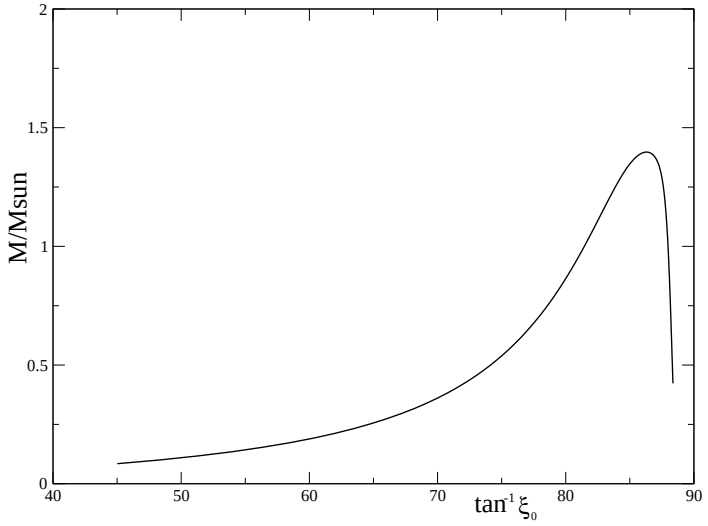

Figure 3: Dependence of mass M on ξ_0 for Helium white dwarf stars.

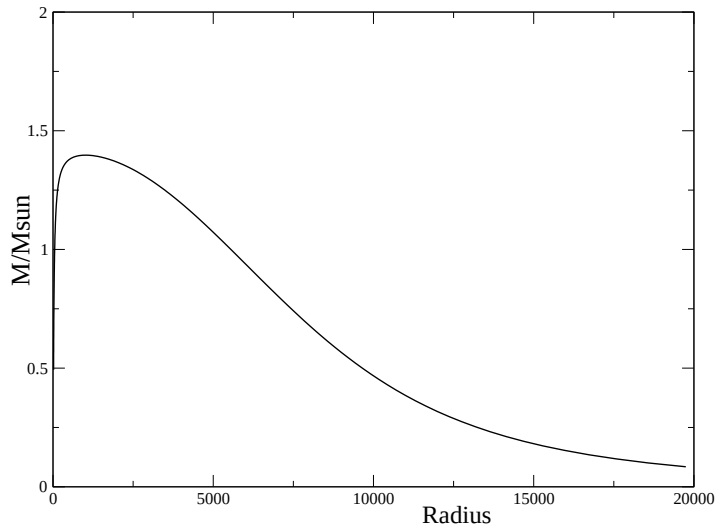

Figure 4: Mass-Radius relationship for Helium white dwarf stars.

We also solve the TOV equations for iron white dwarf stars (for which $\mu_e = 2.154$) and obtain the corresponding mass-radius relationship. Fig. 5 shows the occurance of the critical limiting mass for iron white dwarfs, giving the critical mass to be $1.204\, M_{\odot}$.

The critical central densities for a few white dwarf stars are also computed numerically based on the TOV equation [(12) and (13)] and the results are shown in Column 2 of Table 2.

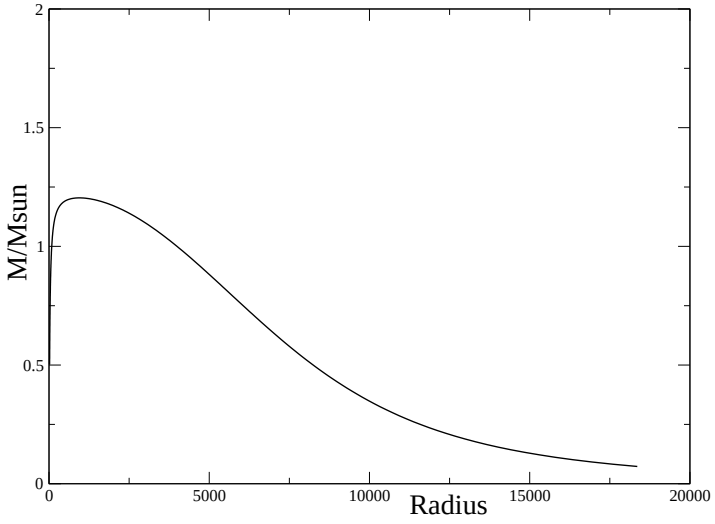

Figure 5: Mass-Radius relationship for Iron white dwarf stars.

4.2 Inverse Beta Decay Instability

The process of inverse beta-decay, namely

$$ {}^{A}_{Z}X + e \longrightarrow {}^{A}_{Z-1}Y + \nu_e $$

becomes important for high values of electron density. Usually this fact is ignored when calculating the most stable configuration of white dwarfs. At high electron densities, the elctrons become more relativistic so that the condition $E_F \geqslant \epsilon_z$, where E_F is the fermi energy and ϵ_z is the difference in binding energies of the parent and daughter nuclei, may be satisfied for inverse beta-decay to occur.

At a high density, the star becomes unstable under inverse beta-deacay and collaspes to form much dense matter (this might be a mixture of neutron rich nuclei, electrons and neutrons). The threshold density for inverse beta-decay was calculated [27, 28] by setting $E_F = \epsilon_z$. This gives

$$ \rho_N = \frac{\mu_e H}{3\pi^2\hbar^3 c^3}(\epsilon_z^2 + 2m_e c^2 \epsilon_z)^{3/2} \tag{22} $$

where beta-decay energy ϵ_z is obtained experimentally and is listed in Ref. [29]. The values of the neutronization threshold densities ρ_N following from Eq. (22) are listed in Column 4 of Table 2.

For white dwarfs whose neutronization density is smaller than the onset density of gravitational instability we expect an unstable phase before reaching the critical mass obtained from general relativity. Inverse beta-decay that sets in before the gravitational instability reduces the electron density which in turn reduces the degeneracy pressure so that we expect a smaller value for critical mass than that obtained by general relativity. Table 2 compares the critical central density and inverse beta-decay threshold density for white dwarfs of different compositions. Critical central density given in the second columm is obtained by solving Eqs. (12) and (13) for $\mu_e = 2$ (for ${}^{4}_{2}$He, ${}^{12}_{6}$C, ${}^{16}_{8}$O, ${}^{20}_{10}$Ne, ${}^{24}_{12}$Mg, ${}^{28}_{14}$Si, and ${}^{32}_{16}$S) and $\mu_e = 2.154$ (for ${}^{56}_{26}$Fe). These values are expected to be better than the values given in the third column [obtained from Eq. (21)] as they are based on the solution of the full TOV equation.

Table 2: Critical values in general relativity and neutronization for different white dwarfs. Here ρ_c is the critical central density in general relativity, $\rho_c^{\rm pre}$ is the preivous estimate [26] of the critical central density, ρ_N is the neutronization threshold density. M_c is the limiting mass of the star following from the solution of the TOV equation with the corresponding central density ρ_c. M_N is the neutronization threshold mass of the star following from the solution of the TOV equation with the corresponding neutronization density ρ_N taken as the central density.

	ρ_c in g/cm^3	$\rho_c^{\rm pre}$ in g/cm^3	ρ_N in g/cm^3	M_c in $M_\odot$	M_N in $M_\odot$
$^4_2$He	2.3588×10^{10}	2.65×10^{10}	1.3728×10^{11}	1.397	—
$^{12}_6$C	2.3588×10^{10}	2.65×10^{10}	3.9004×10^{10}	1.397	—
$^{16}_8$O	2.3588×10^{10}	2.65×10^{10}	1.9018×10^{10}	1.397	1.396
$^{20}_{10}$Ne	2.3588×10^{10}	2.65×10^{10}	6.2134×10^{9}	1.397	1.389
$^{24}_{12}$Mg	2.3588×10^{10}	2.65×10^{10}	3.1599×10^{9}	1.397	1.380
$^{28}_{14}$Si	2.3588×10^{10}	2.65×10^{10}	1.9712×10^{9}	1.397	1.365
$^{32}_{16}$S	2.3588×10^{10}	2.65×10^{10}	1.4755×10^{8}	1.397	1.202
$^{56}_{26}$Fe	2.5718×10^{10}	3.07×10^{10}	1.1452×10^{9}	1.204	1.157

Comparing the critical densities given in the second and fourth columns of Table 2, we see, for $^4_2$He and $^{12}_6$C white dwarf stars, that gravitational instability sets in before neutronization instability can set in. This implies that the critical mass for helium and carbon white dwarf stars is $1.397\,M_\odot$. For all the rest of the stars, threshold density for neutronization starts before the critical density for gravitational instability is reached. This implies the critical masses of $^{16}_8$O, $^{20}_{10}$Ne, $^{24}_{12}$Mg, $^{28}_{14}$Si, and $^{32}_{16}$S white dwarf stars must be lower than $1.397\,M_\odot$ and the critical mass of $^{56}_{26}$Fe white dwarf stars must be lower than $1.204\,M_\odot$. We compute the corresponding masses numerically from the TOV equations and identify them as the critical masses for stability aganist neutronization, which are shown in the last column of Table 2.

5 Conclusions

From our above investigation it has been seen that the general relativistic effects have lowered the limiting mass of a white dwarf star. The new value ($1.397\,M_\odot$) that is obtained by solving the Tolman-Oppenheimer-Volkoff equation is not too far from Chandrasekhar's limit ($1.452\,M_\odot$). Thus it is clear that the general relativistic effects are small in the case of a white dwarf star that lowers the Chandrasekhar's limit by approximately 4%.

The equation of state we assumed is valid for all electron velocities, both non-relativistic and ultra relativistic, connecting the two regimes smoothly. However, the equation of state does not incorporate the inter-particle interaction. The neglect of inter-particle interaction is however justified in the limit of high density [15]. In fact it was shown in Ref. [17] that the electrostatic correction to the equation of state can be treated as negligible. The maxima of the mass-radius curve (in Fig. 4) marks the onset of gravitational collapse and the region towards the left of the maxima corresponds to an unstable region. It is expected that the growth in density makes the electrons more relativistic

so that the condition favoring inverse beta decay is approached.

We took account of the neutronization by using Eq. (22) obtained on the basis of Salpeter's arguments and calculated the onset density for inverse beta-decay for different compositions of the star (shown in Column 4 of Table 2). We found that stars composed of lighter elements ($^4_2$He and $^{12}_6$C) are more stable than those composed of heavier elements ($^{16}_8$O, $^{20}_{10}$Ne, $^{24}_{12}$Mg, $^{28}_{14}$Si, $^{32}_{16}$S and $^{56}_{26}$Fe). The onset for inverse beta decay is found to start before reaching the onset of gravitaional instability in the heavier elements. The maximum stable mass we obtained by solving TOV equations for these stars ($1.397\,M_\odot$ for $^{16}_8$O, $^{20}_{10}$Ne, $^{24}_{12}$Mg, $^{28}_{14}$Si, $^{32}_{16}$S and $1.204\,M_\odot$ for $^{56}_{26}$Fe) no longer can be indentified as the limiting masses. In the last column of Table 2, we list the maximum stable mass by solving the TOV equations corresponding to the central densities for neutronization thresholds.

Mass distribution of a large number of white dwarf stars with a wide range of masses, including low and massive stars, were ploted by various researchers [31, 32]. The most massive non-magnetic white dwarf observed was LHS4033 [30, 31, 32] which was predicted to have an oxygen-neon core with a mass in the range of 1.318—$1.335\,M_\odot$. This range of mass values is consistent with our calculations as we see from the last column of Table 2.

Acknowledgement

The computational work was performed at the Numerical Lab., Department of Physics, Indian Institute of Technology Guwahati.

References

[1] F. W. Dyson, A. S. Eddington and C. Davidson, Philos. Trans. Roy. Soc. (London) **220A**, 291 (1919).

[2] R. V. Pound and G. A. Rebka, Phys. Rev. Lett. **3**, 439 (1959).

[3] R. V. Pound and J. L. Snider, Phys. Rev. **140**, B788 (1965).

[4] K. Huang, *Statistical Mechanics*, John Wiley (1987).

[5] P. Dirac, Proc. R. Soc. **A 112**, 661 (1926).

[6] R. H. Fowler, Mon. Not. Roy. Astro. Soc. **87** ,114 (1926).

[7] W. Anderson, Z. Phys. **1**, 851 (1929).

[8] E. C. Stoner, Philos. Mag. **7**, 63 (1929); **9**, 944 (1930).

[9] S. Chandrasekhar, Astrophys. J. **74**, 81 (1931).

[10] S. Chandrasekhar, M.N., **91**, 456 (1931).

[11] S. Chandrasekhar, M.N., **95**, 207 (1935).

[12] S. Chandrasekhar, *Introduction to the Study of Stellar Structure*, University of Chicago Press (1939).

[13] S. Chandrasekhar, ApJ. **139**, 1396 (1964).

[14] S. P. S. Anand, Proc. Nat. Acad. Sci. **54**, 23 (1965).

[15] L. D. Landau and E. M. Lifshitz, *Statistical Physics*, Part 1, 3rd Ed., Butterworth-Heinemann (1980).

[16] D. Bohm and D. Pines, Phys. Rev. **82**, 625 (1951).

[17] R. P. Singh, Astrophys. J., **126**, 213 (1957).

[18] R. C. Tolman, Phys. Rev. **55**, 364 (1939).

[19] J. R. Oppenheimer and G. M. Volkoff, Phys. Rev. **55**, 374 (1939).

[20] Recalculation of the Chandrasekhar's limit by numerical integration of the Newtonian equations (18) and (19) yields $1.452\,M_{\odot}$.

[21] R. C. Tolman, *Relativity, Thermodynamics and Cosmology*, Oxford University Press (1958).

[22] L. D. Landau and E. M. Lifshitz, *Classical Theory of Fields*, 4th Ed., Butterworth-Heinemann (1975).

[23] C. W. Misner, K. S. Thorne, and J. A. Wheeler, *Gravitation*, Freeman (1973).

[24] N. Straumann, *General Relativity and Relativistic Astrophysics*, Springer-Verlag (1984).

[25] Ya. B. Zeldovich and I. D. Novikov, *Stars and Relativity*, Dover (1971).

[26] S. L. Shapiro and S. A. Teukolsky, *Black Holes, White Dwarfs, and Neutron Stars—The Physics of Compact Objects*, John Wiley (1983).

[27] E. E. Salpeter, Astrophys. J. **134**, 669 (1961).

[28] J. A. Rueda, M. Rotondo, R. Ruffini and S. S. Xue, arXiv:1012.0154v1 [astro-ph.SR] (2010).

[29] A. G. W. Cameron, *Chalk River Rept.* CRP-690 (1957).

[30] C. C. Dahn, P. Bergeron, J. Liebert , H. C. Harris, B. Canzian, S. K. Leggett, S. Boudreault, Astrophys. J. **605**, 400 (2004).

[31] P. Bergeron, A. Gianninas, and S. Boudreault, arXiv:astro-ph/0611904v1 (2009).

[32] S. O. Kepler, S. J. Kleinman, A. Nitta, D. Koester, B. G. Castanheira, O. Giovannini, A. F. M. Costa and L. Althaus, Mon. Not. R. Astron. Soc. **375**, 1315 (2007).